ACS OMEGA

http://pubs.acs.org/journal/acsodf

Article

Study on the Strengthening Mechanism of a MIBC−PEG Mixed Surfactant on Foam Stability

Mengdi Xu, Fangyu Guo, Xicheng Bao, Xiahui Gui, Yaowen Xing,* and Yijun Cao

Cite This: *ACS Omega* 2023, 8, 27429−27438

Read Online

ACCESS | Metrics & More | Article Recommendations

ABSTRACT: In the flotation process, the frother, which is typically a surfactant, can be added to the pulp to reduce the surface tension and create stable foam. Currently, the nonionic mixed surfactant is widely employed as the frother for fine coal flotation. In this study, we focused on examining the foam properties of a mixed surfactant comprising short-chain methyl isobutyl carbinol (MIBC) and long-chain polyethylene glycol-1000 (PEG). Analytical techniques such as surface tension measurement, dynamic foam stability measurement, bubble morphology observation, and foam film drainage measurement were used to investigate the foam properties in single and mixed surfactant solution from a macroscopic scale to a microscopic scale. The surface tension results indicated that PEG exhibited higher surface activity than MIBC, and the addition of PEG to MIBC resulted in a significant reduction in solution surface tension. The dynamic foam stability analysis revealed that the incorporation of a small amount of PEG into MIBC solution notably improved foam stability. Furthermore, the addition of PEG to the MIBC solution led to a shift in the bubble size distribution curve from a "double peak" to a "single peak" shape. This shift indicated a substantial reduction in bubble size, indicating an enhanced inhibition of bubble coalescence. Additionally, the liquid film drainage rate was significantly slowed down, and the stability of the liquid film was improved upon the addition of PEG to MIBC. This improvement can be attributed to the synergistic effect of MIBC and PEG molecules adsorbed at the gas−liquid interface. The synergistic effect of mixed MIBC−PEG was due to the additional surface tension gradient created by the difference in surface activity between PEG and MIBC. This surface tension gradient enhances the Marangoni flow of surfactant molecules, thereby improving the self-healing ability of the liquid film and increasing its stability.

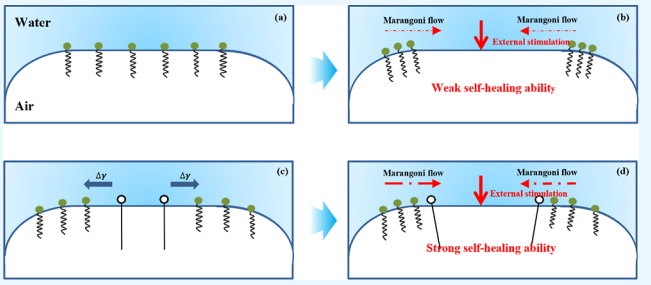

1. INTRODUCTION

Froth flotation is the most effective method of fine coal upgrading due to its selective separation based on differences in surface wettability.[1−6] In the flotation process, hydrophobic particles are trapped by bubbles and continue to rise through the froth layer to the launders, while gangue particles with poor hydrophobicity return to the pulp with the downward flow due to continuous coalescence and dehydration of bubbles in the foam layer, resulting in secondary enrichment. Consequently, the establishment of a precisely controlled and stable froth is crucial for achieving high flotation efficiency and desired product quality.[7−9]

Froth is a highly complex phenomenon influenced by multiple factors.[8,9] In fine coal flotation, the stability of the froth is significantly affected by particles and flotation reagents, namely, frothers and collectors.[10−12] Frothers play a crucial role in facilitating the dispersion of air into fine bubbles and stabilizing the froth.[13−15] They are commonly recognized as surfactants capable of adsorbing at the gas−liquid interface, thereby inducing changes in interface properties, including surface tension, intermolecular forces, charge, and rheology.[16,17] These modifications in surface properties ultimately have an impact on froth stability. In general, the bubble stabilization mechanism of surfactants can be summarized as follows: the adsorption of surfactants on the gas−liquid interface effectively decreases the gas−liquid interfacial tension. This reduction in interfacial tension contributes to the overall stability of the system by lowering the system's energy.[18] The presence of surfactants also leads to a reduction in Laplace pressure, which in turn decreases the driving force for liquid film drainage. As a result, the rate of liquid film drainage is reduced. Furthermore, the adsorption of surfactants at the gas−liquid interface enhances the Gibbs−Marangoni effect.[19,20] This effect strengthens the elasticity of the liquid film, further contributing to the stabilization of the system.

Received: April 26, 2023
Accepted: June 29, 2023
Published: July 19, 2023

The influence of surfactant concentration and type on foam stability can be evaluated by bubble size, and there exists a critical coalescence concentration (CCC) of surfactant on bubble size. When the surfactant concentration is lower than CCC, the increase in surfactant concentration leads to a reduction in bubble size, since the surfactant could inhibit the bubble coalescence. However, once the surfactant concentration surpasses the CCC, further increases in concentration do not cause significant changes in the average bubble size.[21,22] Laskowski et al.[23] correlated the CCC with the dynamic bubble index, and proposed that bubble coalescence under dynamic conditions would affect the stability of bubbles. The investigation of mixed surfactants and their impact on foam stability has emerged as a significant research topic in recent years. Alcohol-based foaming agents are extensively utilized as frothers in fine coal flotation. Among alcohol-based foaming agents, the foam formed by alkanols with short chains has poor foam stability, resulting in good selectivity of fine coal flotation but high agent consumption. The foam formed by alkanols with long chains has a strong foaming ability, resulting in poor selectivity and small agent consumption. Currently, nonionic mixed surfactant represented by miscellaneous alcohols are most commonly used foaming agents of fine coal flotation. Compared with single surfactant, mixed surfactant creates higher flotation efficiency. Gupta et al.[24] found that mixed alcohols and pegylated surfactants have a certain synergistic strengthening effect on fine coal flotation, which was because the mixture of alcohols and pegylated has stronger surface activity and ability to decrease the surface tension. Tan et al.[25] reported that a synergistic effect occurred in a mixture of low molecular weight and high molecular weight polypropylene glycols system, resulting in an increase in foam height compared to the performance of individual systems. This result indicated that the improvement of foam stability is due to the increase in elasticity of the gas−liquid interface and thus inhibit bubble coalescence. Laskowski et al.[23] observed that the foam stability in mixed methyl isobutyl carbinol (MIBC) and Dowfroth is better than that in single MIBC, while lower than that in single Dowfroth. Dey et al.[26] has shown that the foam stability in a mixed system of MIBC and PEG was between that of the two single surfactants. When MIBC and PEG were mixed at a ratio of 9:1, the flotation recovery and selectivity of fine coal increased significantly, which was mainly due to the synergistic adsorption of two surfactants at the gas−liquid interface. The enhancement of foam stability can be achieved by augmenting the Marangoni effect at the gas−liquid interface. In recent years, the mixed surfactant could enhance the foam stability through synergistic adsorption has been reached a consensus. However, the stabilization mechanism of mixed surfactant based on foam film drainage between bubbles at the micro scale is not clear, and requires a further investigation.

In the present study, we conducted surface tension measurement, dynamic foam stability measurement, bubble morphology observation, and foam film drainage measurement to investigate the effect of mixed surfactant with long and short chains on foam stability and to provide a comprehensive understanding of the underlying strengthening mechanism. The results of this study will offer guidance for the regulation of foam stability in flotation processes.

2. EXPERIMENTAL SECTION

2.1. Materials. In this investigation, the effects of mixed surfactant on foam stability were explored, with particular emphasis on the utilization of short-chain alcohol MIBC and long-chain alcohol PEG as the selected compounds for study. Both analytical-grade MIBC and PEG were obtained from Aladdin Chemical Company (Shanghai, China), and Milli-Q water was used to prepare the solutions. The mixed surfactant solutions were prepared by blending varying proportions of MIBC and PEG.

2.2. Surface Tension Measurement. The surface tension of the surfactant solution was measured using an automatic surface tension meter (K100, KRUSS). Both single and mixed surfactant solutions were homogeneously oscillated using an ultrasonic instrument before the measurements. The instrument operates based on the puller method. The platinum sheet used was thoroughly cleaned with Milli-Q water before the test and burned with an alcohol lamp to eliminate potential interference. Each experiment was conducted three times at a temperature of 20 °C to ensure accuracy.

2.3. Dynamic Foam Stability Measurement. Foam stability can be evaluated through dynamic and static tests.[27,28] In a dynamic test, foam growth and decay achieve a state of dynamic equilibrium, whereas static test primarily observe the foam collapse process after inflation, with the foam growth rate being zero. Typically, a combination of both tests is used to assess foam stability, with the maximum height and half-life of the foam layer serving as indicators.[29,30] The Bikerman airflow method was utilized in this study to measure foam stability using a foam column.[31−33] Each experiment was repeated thrice to ensure the results fell within a reasonable error margin.

2.4. Bubble Morphology and Size Distribution Measurement. This system was established to observe the bubble morphology and size distribution in various surfactant solutions. During testing, 100 mL of surfactant solution was aerated at a fixed rate using an air pump, and the resulting bubbles were observed and recorded with a high-speed dynamic camera. Image-Pro Plus software was used to analyze the images of bubbles. The images were preprocessed by adjusting the grayscale and contrast and intensity to enhance the clarity of the bubbles in the images. After identification of the bubbles, geometric parameters were set, the actual bubble size was calculated, and the distribution of bubble size was analyzed.

2.5. Foam Film Drainage Measurement. The dynamic film apparatus system (DFA) was employed to examine foam film drainage. This system consisted of an inverted optical microscope (IX73, Olympus, Japan), a high-speed dynamic camera for interference (I-speed 221, iX Cameras, UK), a high-speed dynamic camera for side view (Optimos, OImaging, Canada), and a bubble generation and drive unit. The sequential interference fringes (Newton rings) during the liquid film drainage process were recorded and later analyzed with MATLAB software to understand the mechanism of liquid film drainage and rupture. Prior to experiments, the glass cell bottom was hydrophobized using octadecyl trichlorosilane, and both the glass cell and capillary were meticulously cleaned to ensure the generation of clean bubbles. A single bubble with a diameter of 3 mm was formed at the base of the glass cell using a micro-syringe. Subsequently, a similarly sized bubble was produced at the tip of the capillary tube. A piezo actuator

https://doi.org/10.1021/acsomega.3c02863
ACS Omega 2023, 8, 27429−27438

was used to discharge the extra solution between the two bubbles, thereby creating a horizontal foam film. The time-dependent drainage of this foam film was observed using monochromatic interference microscopy. Subsequent processing of the interference fringes through MATLAB software provided the dynamics of the foam film and film thickness. For each test, the two bubbles started from the same initial position. Each group of tests was repeated at least two times.

3. RESULTS AND DISCUSSION

3.1. Surface Tension Results. The effect of MIBC, PEG concentration, and the ratio of MIBC−PEG mixed surfactant on surface tension of solution was investigated, as shown in Figure 1. The surface tension of Milli-Q water at room temperature was found to be 72.48 mN/m. It was observed that the surface tension decreased with the increase in surfactant concentration, albeit at varying magnitudes, indicating differences in the surface activity of the surfactants. At a surfactant concentration of 10^{-5} mol/L, the surface tension of MIBC was found to be 72.46 mN/m, which was similar to that of Milli-Q water. With an increase in MIBC concentration to 5×10^{-5}, 10^{-4}, 5×10^{-4}, and 10^{-3} mol/L, the surface tension decreased to 72.43, 72.28, 71.22, and 70.56 mN/m, respectively. Similarly, for PEG, at a surfactant concentration of 10^{-5} mol/L, the surface tension was 68.68 mN/m. As the PEG concentration increased to 5×10^{-5}, 10^{-4}, 5×10^{-4}, and 10^{-3} mol/L, the surface tension significantly decreased to 67.84, 67.26, 66.32, and 65.21 mN/m. This indicated that PEG exhibits higher surface activity compared to MIBC.

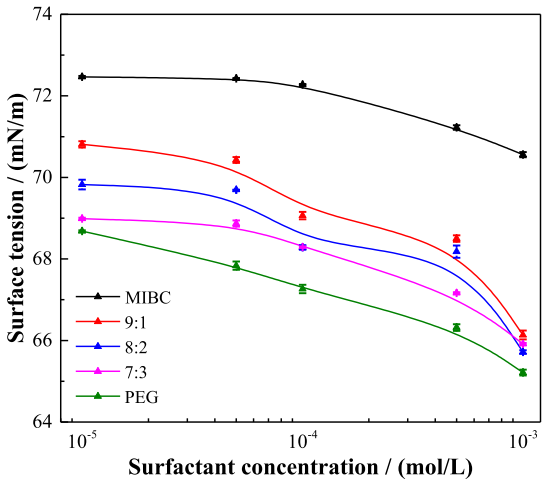

Figure 1. Effect of MIBC, PEG concentration, and ratio of MIBC−PEG mixed surfactant on surface tension of solution.

When PEG was added to the MIBC solution, the surface tension of the mixed solution decreased as the surfactant concentration increased. It was observed that, under the same concentration condition, the surface tension of the mixed solution was lower than that of single MIBC solution. Furthermore, the extent of surface tension reduction increased with a higher proportion of PEG in the mixture. For instance, in the case of a mixed surfactant solution with a ratio of 9:1 (MIBC−PEG), the surface tension measured 70.81 mN/m at a surfactant concentration of 10^{-5} mol/L. As the ratio was increased to 8:2 and 7:3, the surface tension of mixed surfactant solution decreased to 69.83 and 68.99 mN/m, respectively. The same trend was also observed as the surfactant concentration was increased to 5×10^{-5}, 10^{-4}, 5×10^{-4}, and 10^{-3} mol/L. These findings suggested that PEG being a powerful surfactant reduces the surface tension more readily than MIBC and the presence of it in a very small quantity in a mixture causes high surface tension gradient due to the different adsorption capacity of the frother molecules at the gas−liquid interface.

3.2. Dynamic Foam Stability Results. The effect of MIBC and PEG at concentrations of 20, 40, 80, and 120 ppm on maximum foam height was investigated using a foam stability test device, as illustrated in Figure 2. The results indicated that the maximum foam height of both MIBC and PEG increased with higher surfactant concentrations. At the surfactant concentration of 20 ppm, the maximum foam height was 7.64 cm for MIBC and 10.10 cm for PEG. At higher MIBC concentrations of 40, 80, and 120 ppm, the maximum foam height increased to 9.70, 11.40, and 13.30 cm, respectively. Similarly, at higher PEG concentrations of 40, 80, and 120 ppm, the maximum foam height increased to 18.63, 19.32, and 20.95 cm, respectively. The maximum foam height serves as an indicator of the foaming ability of surfactant solutions, which in this case demonstrated an increase with higher surfactant

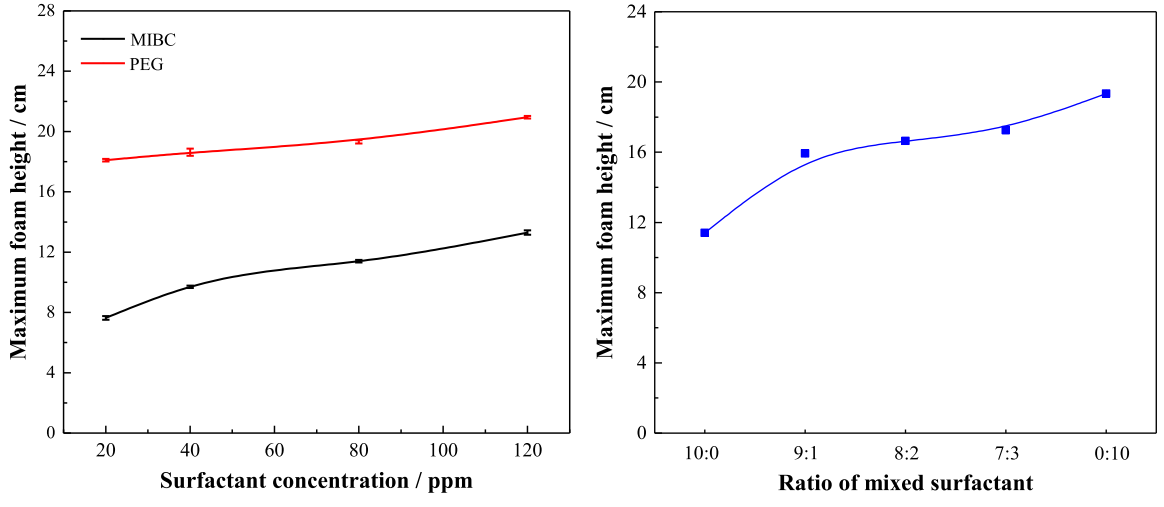

Figure 2. Effect of MIBC, PEG concentration, and ratio of MIBC−PEG mixed surfactant on maximum foam height.

https://doi.org/10.1021/acsomega.3c02863
ACS Omega 2023, 8, 27429−27438

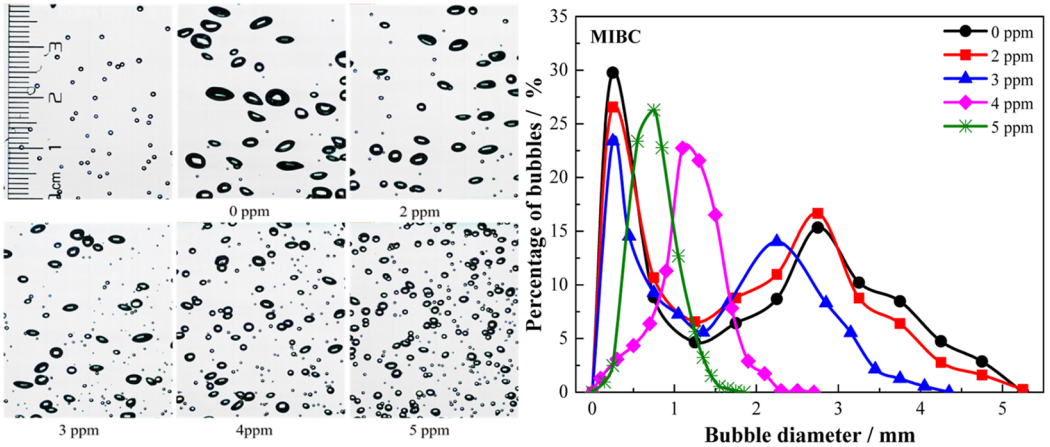

Figure 3. Bubble morphology and size distribution in MIBC solution.

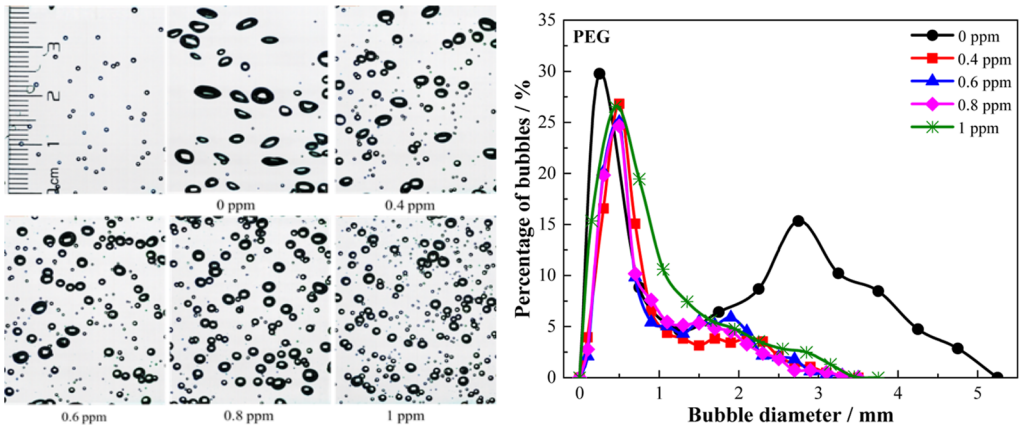

Figure 4. Bubble morphology and size distribution in PEG solution.

concentration. Comparing the maximum foam heights of MIBC and PEG solutions, PEG exhibited a stronger foaming ability. Additionally, at a surfactant concentration of 80 ppm, the maximum foam height of mixed surfactant with different mass ratios is also presented in Figure 2. The observed maximum foam height was 11.40 cm when PEG was not added to the MIBC solution. As the mass ratio of PEG in the MIBC solution increased, the maximum foam height also increased. At a ratio of 9:1 (MIBC−PEG), the maximum foam height was 8.66 cm, and as the ratio increased to 7:3, the maximum foam height increased to 12.65 cm. This suggested that a mixture of MIBC and PEG could enhance the foaming ability of the solution compared to using single MIBC.

The foam half-life of MIBC and PEG at concentrations of 20, 40, 80, and 120 ppm was recorded. At a concentration of 20 ppm, the foam half-life was 6.95 s for MIBC and 11.4 s for PEG. As the concentration of MIBC increased to 40, 80, and 120 ppm, the foam half-life increased to 6.08, 7.00, and 8.32 s, respectively. Similarly, as the concentration of PEG increased to 40, 80, and 120 ppm, the foam half-life increased to 11.70, 12.65, and 12.77 s, respectively. Foam half-life is a crucial parameter for evaluating the stability of surfactant solutions, and it is evident that foam stability improved with higher surfactant concentration. Furthermore, the foam stability of PEG was found to be stronger than that of MIBC. Additionally, the foam half-life of mixed surfactant with different ratios at a concentration of 80 ppm was also recorded. The foam half-life of the MIBC solution without PEG was 6.95 s. As the ratio of MIBC to PEG increased from 9:1 to 7:3, the foam half-life increased to 8.67 and 10.64 s, respectively. These results suggested that the mixture of short-chain alcohol MIBC and long-chain alcohol PEG enhanced the foam stability of the solution compared to the use of MIBC alone.

3.3. Bubble Morphology Observation. The present study employed a bubble morphology observation system to capture images of bubble morphology in surfactant solutions. The acquired images were then analyzed using Image-Pro Plus software to calculate bubble diameter and size distribution curves in both Milli-Q water and surfactant solutions. The effect of MIBC concentration on bubble morphology and size distribution is depicted in Figure 3. In Milli-Q water, the large bubbles displayed a flattened shape, whereas the small bubbles were spherical. The curve representing the distribution of bubble sizes exhibited a "double peak" shape, indicating a higher proportion of large and small bubbles, with a relatively lower number of middle-sized bubbles. This outcome can be attributed to the strong bubble coalescence phenomenon in Milli-Q water, where the coalescence of bubbles often results in the formation of smaller bubbles around the newly formed larger bubble, referred to as "child bubbles". Tse et al.[34,35] suggested that the release of dynamic energy diffusing around the bubble in the form of an annular wave during bubble coalescence can lead to the formation of a small bubble around the large bubble. Additionally, an unstable extension on the bubble's surface and the separation of a small portion of gas

https://doi.org/10.1021/acsomega.3c02863
ACS Omega 2023, 8, 27429−27438

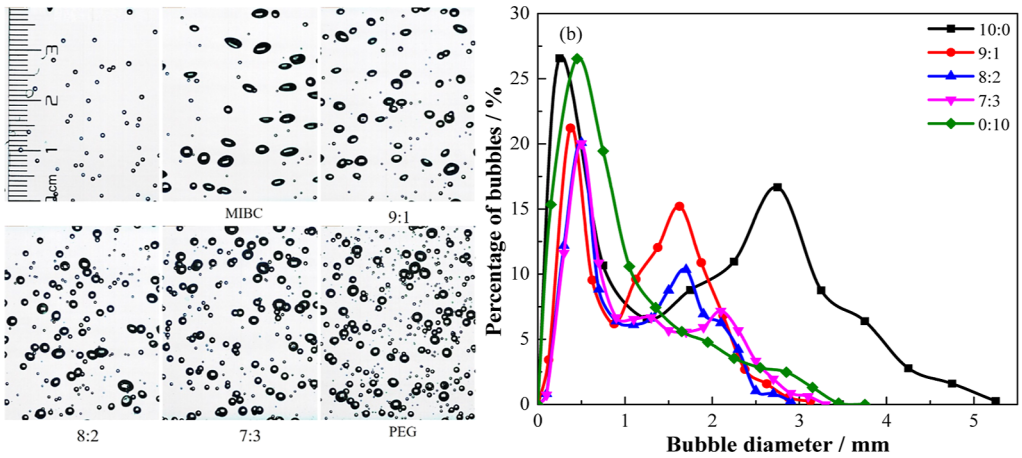

Figure 5. Bubble morphology and size distribution in MIBC and PEG mixture solution.

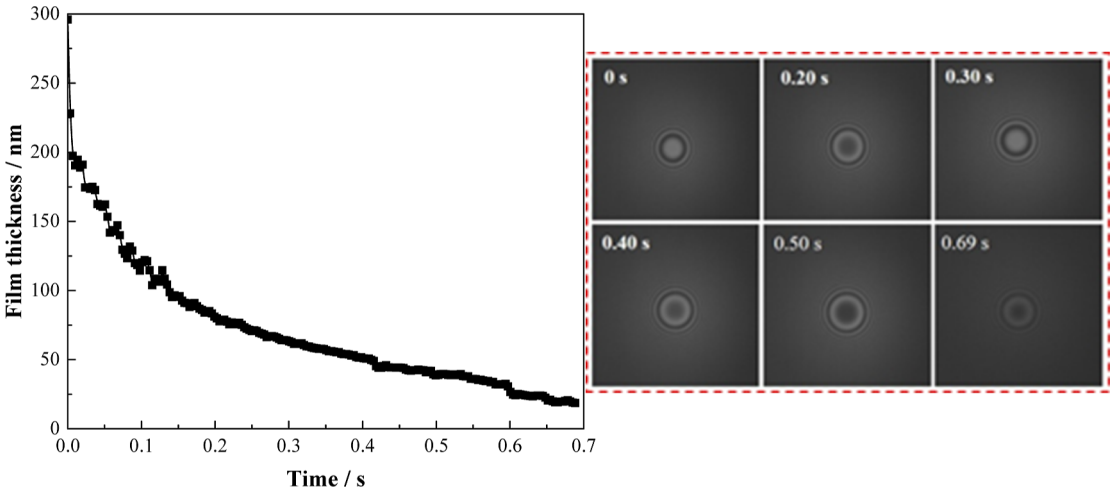

Figure 6. (Left) Dynamics of drainage at the central point of foam film in Milli-Q water. (Right) Interference images of film corresponding to each curve in the figure on the left.

form smaller bubbles when the annular wave reached the end of the bubble. Consequently, the more significant the bubble coalescence in the solution, the greater the number of "child bubbles" and the larger the size of newly formed bubbles after coalescence.

In MIBC solution, the bubble size was large and predominantly flat at lower concentration. However, as the MIBC concentration increased, the number of bubbles increased, while the size of bubbles decreased. The shape of bubbles gradually became more spherical. At low MIBC concentrations, the distribution of bubble sizes remained unchanged, displaying a "double peak" shape. As MIBC concentration increased, the peaks of the "double peaks" gradually shifted to the center, ultimately forming a "single peak" size distribution curve at the concentration of 4 ppm. This transition in bubble size distribution indicated that the increase in MIBC concentration effectively inhibited bubble coalescence, resulting in a higher number of middle-sized bubbles. This observation suggested that MIBC played a crucial role in controlling the size distribution of bubbles, enhancing foam stability.

The effect of PEG concentration on bubble morphology distribution of bubble size is depicted in Figure 4. The bubble size distribution curve for PEG solutions consistently exhibited a "single peak" shape, and small bubbles were dominant in solution. At a concentration of 0.4 ppm, the bubble size distribution reached a stable level with no significant change observed as PEG concentration increased. This suggested that PEG can effectively inhibit bubble coalescence at lower concentrations, as also reported by Dey.[26] Comparatively, PEG demonstrated a greater ability to inhibit bubble coalescence than MIBC, consistent with the variations observed in surface tension and foam stability.

When a mixed surfactant concentration of 2 ppm was used, the effect of MIBC and PEG mixed solution on bubble morphology and size distribution was examined, as shown in Figure 5. The addition of PEG to the MIBC solution significantly altered the bubble morphology. When the ratio was 9:1 (MIBC−PEG), the solution exhibited a low number of bubbles, with a higher proportion of large bubbles. These large bubbles typically had a flattened shape. In contrast, when the ratio was 7:3, there was a significant increase in the number of bubbles. The size of the bubbles decreased, resulting in a reduced proportion of large bubbles and an increased proportion of small bubbles. Additionally, the shape of the bubbles gradually transitions from a flattened shape to a more spherical shape. In the case of the MIBC and PEG mixture, the bubble size distribution curve demonstrated a "double peak" sharp across the three ratios. As the proportion of PEG components in mixed solution increased, the number of large

https://doi.org/10.1021/acsomega.3c02863
ACS Omega 2023, 8, 27429−27438

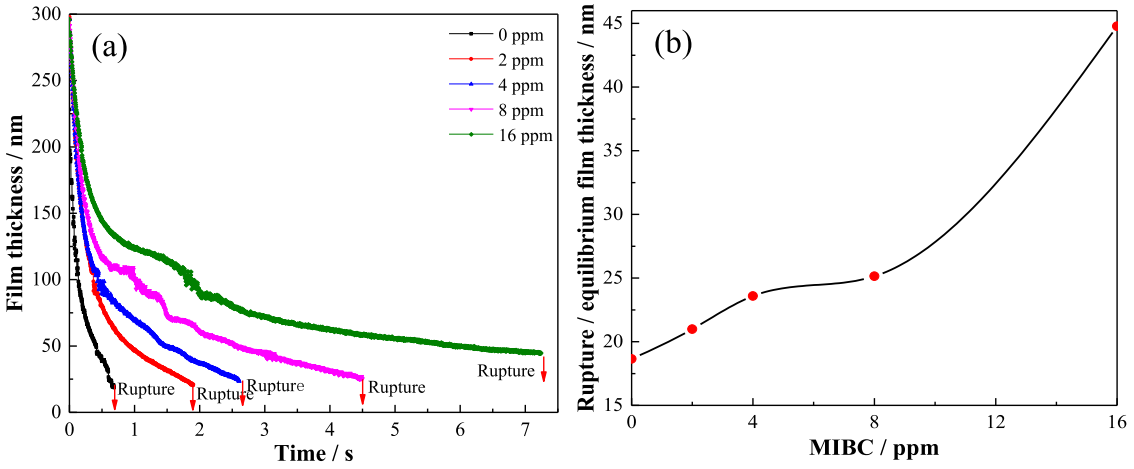

Figure 7. (a) Dynamics of foam film drainage at the thinnest point in different concentrations of MIBC solutions; (b) rupture/equilibrium film thickness of foam film varies with the concentration of MIBC.

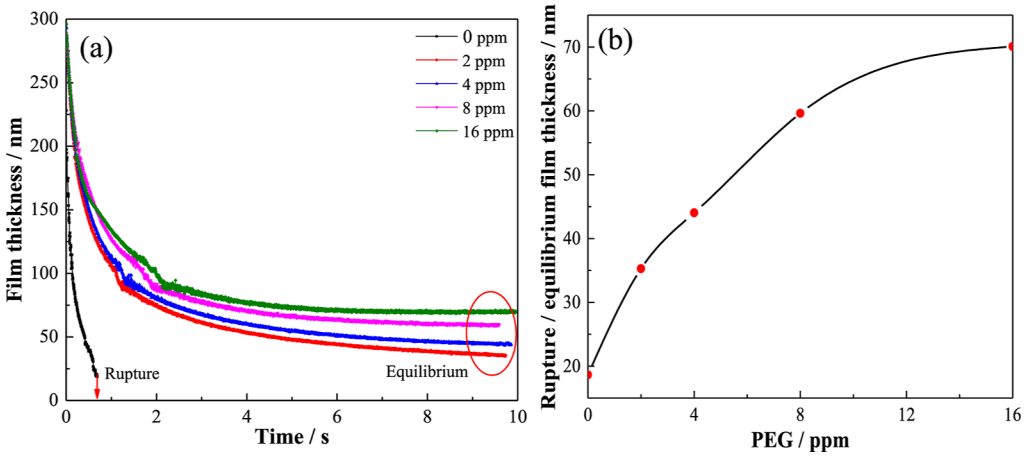

Figure 8. (a) Dynamics of foam film drainage at the thinnest point in different concentrations of PEG solutions; (b) rupture/equilibrium film thickness of foam film varies with the concentration of PEG.

bubbles decreased, while the number of middle-sized bubbles increased, which indicated that the addition of PEG can effectively improve the ability to inhibit bubble coalescence. The mixed surfactant could form a tightly adsorbed layer at the gas−liquid interface, leading to an improved Marangoni effect in the solution. This effect increased the elasticity of the liquid film, allowing for rapid recovery of the deformed liquid and inhibiting bubble coalescence, thus improving foam stability.

3.4. Foam Film Drainage Results. The film drainage and rupture of the microcosmic foam film are essential preconditions for bubble coalescence. To investigate the dynamics of foam film drainage between bubbles, the dynamic film apparatus system (DFA) was employed in this study. The experiments focused on observing the thinning process of liquid films between bubbles in Milli-Q water. The initial moment was defined when the liquid film thickness reached approximately 300 nm. At various time intervals, the thinning dynamics of the liquid film at the central point and the interference imaging of the film were captured. The drainage dynamics at the central point of the foam film in Milli-Q water and the interference images of the film is presented in Figure 6. It was observed that a stable liquid film could not be sustained between two bubbles in Milli-Q water. As the liquid film between the bubbles continued to thin, it eventually ruptured at the central point after 0.69 s, with a critical rupture thickness of 18.65 nm. Previous studies[36,37] have highlighted the presence of hydrophobic forces between bubbles in Milli-Q water, which increase as the thickness of the liquid film decrease. These forces contribute to the instability and ultimate rupture of the liquid film between bubbles. In line with the observations in Figure 6, the rate of liquid film drainage was found to decrease as the film thickness decreased. This can be attributed to the increasing electrostatic repulsion generated by the electric double layers between bubbles as the film thickness diminishes. The enhanced electrostatic repulsion hinders the drainage process, resulting in a reduced rate of liquid film thinning.

The dynamics of foam film drainage at the thinnest point and rupture/equilibrium film thickness of the foam film varies with the concentration of MIBC is presented in Figure 7. In MIBC solution of different concentrations, the liquid film between bubbles consistently exhibited instability and ultimately ruptured after thinning. Compared to Milli-Q water, the addition of MIBC resulted in a decreased liquid film drainage rate. Furthermore, the liquid film drainage rate showed a significant decrease as the MIBC concentration increased. For instance, at the MIBC concentration of 2 ppm, the liquid film ruptured at 1.09 s. As the concentration increased to 4, 8, and 16 ppm, the rupture time increased to 2.61, 4.50, and 7.24 s, respectively. These findings suggested

https://doi.org/10.1021/acsomega.3c02863
ACS Omega 2023, 8, 27429−27438

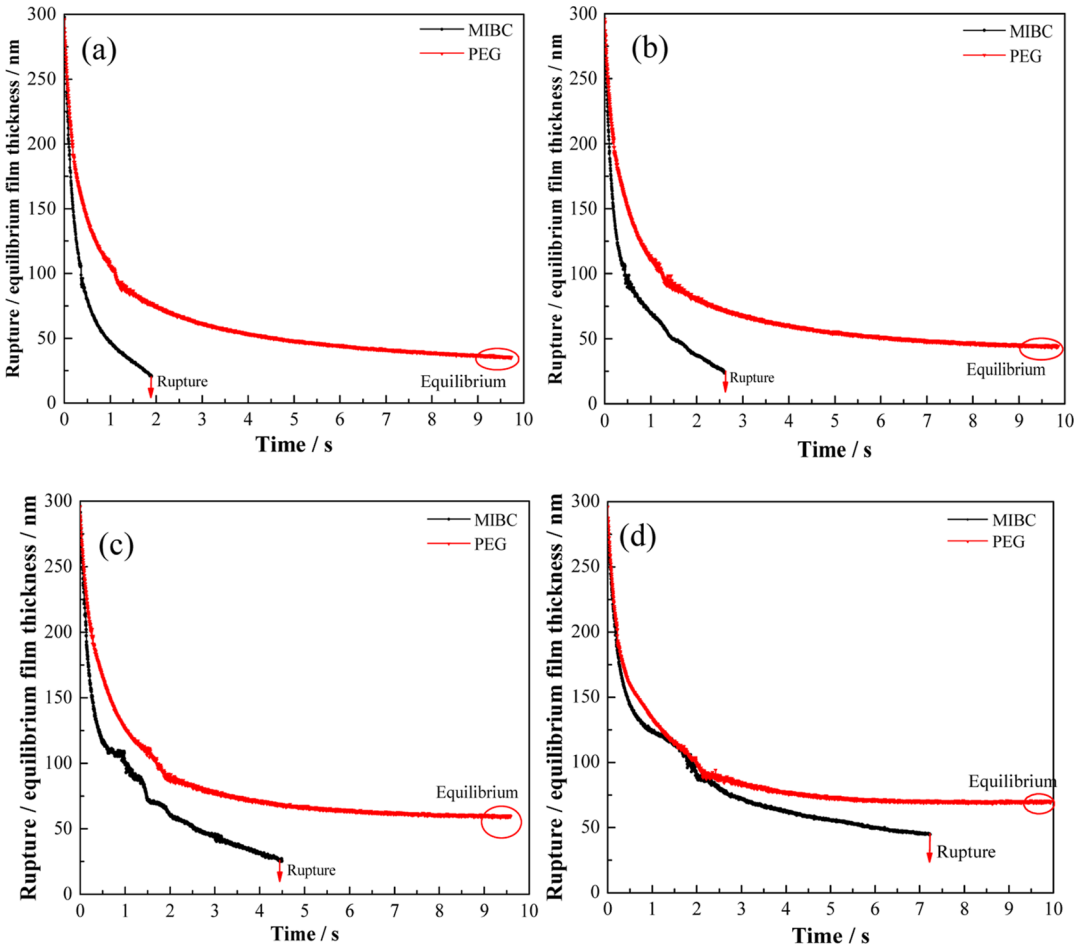

Figure 9. Dynamic of foam film thinning at central point in surfactant solutions of different concentrations, (a) 2, (b) 4, (c) 8, and (d) 16 ppm.

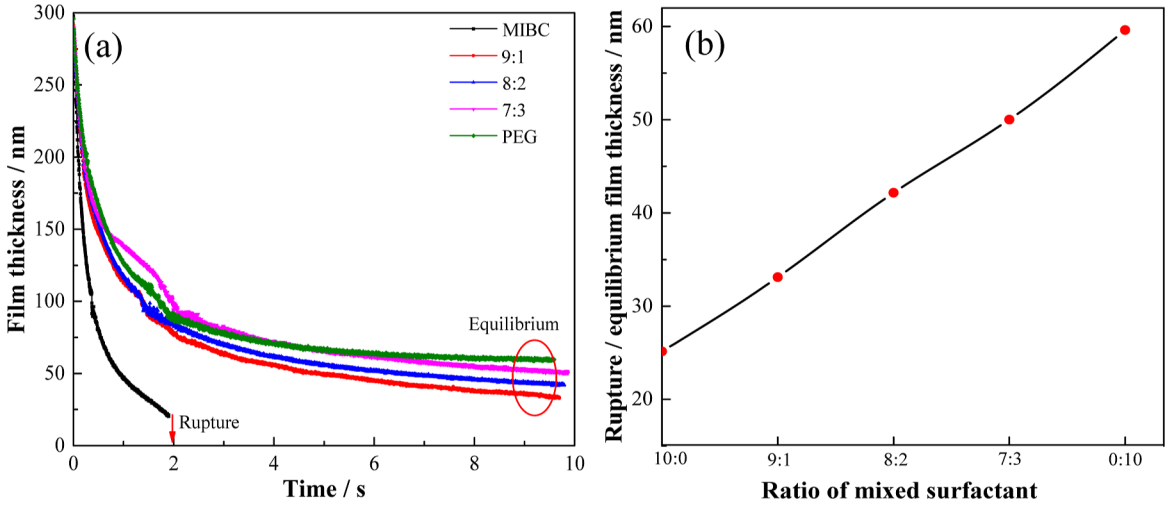

Figure 10. (a) Dynamics of foam film drainage at the thinnest point with different ratios of mixed surfactant; (b) rupture/equilibrium film thickness of the foam film with different ratios of mixed surfactant.

that the inclusion of MIBC can retard the drainage rate of the liquid film and enhance its stability. The critical rupture/equilibrium film thickness of the liquid film increased with an increase in MIBC concentration, which was consistent with the observed change in the liquid film drainage rate. When the concentration of MIBC was lower, the hydrophobic attraction existed between bubbles, resulting in a fast drainage rate of the liquid film. However, as the surfactant concentration increased, the hydrophobic attraction within the system diminishes. Consequently, the drainage rate of the liquid film gradually decreased, leading to an extended rupture time for the liquid film. Ultimately, this enhanced the overall stability of the liquid film.

https://doi.org/10.1021/acsomega.3c02863
ACS Omega 2023, 8, 27429−27438

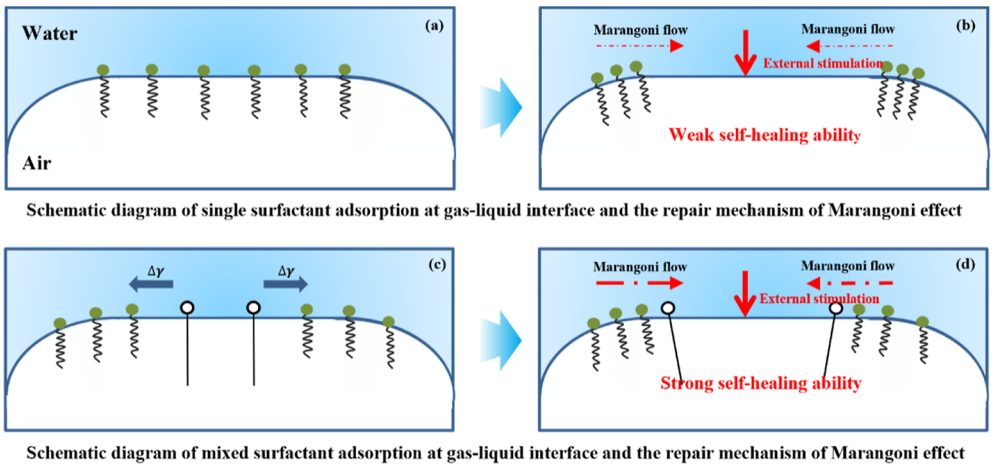

Figure 11. Schematic diagram of single and mixed surfactant adsorption at the gas−liquid interface and the repair mechanism of the Marangoni effect.

The dynamics of foam film drainage at thinnest point and rupture/equilibrium film thickness of foam film varies with the concentration of PEG is presented in Figure 8. In PEG solutions with different concentrations, a stable liquid film was formed between bubbles, which eventually reached equilibrium after drainage. The addition of PEG demonstrated a significant reduction in the drainage rate of the foam film and an improvement in its stability, in comparison to Milli-Q water. As the concentration of PEG increased, the drainage rate of the liquid film decreased. The surface tension of the solution decreased at lower PEG concentrations, resulting in a smaller Laplace pressure between bubbles and a slower liquid film drainage rate. The hydrophobic attraction between bubbles decreased with the increase of PEG concentration, further decreasing the film drainage rate and improving the stability of the liquid film. As the PEG concentration increased from 2 ppm increased to 4, 8, and 16 ppm, the equilibrium film thickness increased from 35.28 to 44.03, 59.62, and 70.09 nm, respectively. This increase in equilibrium film thickness also suggested an increase in the stability of the liquid film with an increase in PEG concentration.

Figure 9 shows a comparison of the dynamics of the liquid film between bubbles in MIBC and PEG solutions at different concentrations. The liquid film drainage rate was slower in PEG solutions than in MIBC solutions with the same surfactant concentration, indicating greater stability of the liquid film between bubbles in PEG solutions. Both PEG and MIBC stabilize the liquid film by reducing the hydrophobic attraction between bubbles. However, the ability of PEG to stabilize the bubbles was stronger than that of MIBC, which is consistent with the results of dynamic foam stability measurement.

Figure 10 presents the dynamics of foam film drainage at the thinnest point, as well as the rupture/equilibrium film thickness of the foam film with different ratios of mixed surfactant when the concentration of the mixed surfactant was 8 ppm. In the MIBC and PEG mixed solutions, the liquid film between bubbles reached an equilibrium state following drainage. Notably, compared to single MIBC solutions, the liquid film drainage rate experienced a significant reduction in the MIBC and PEG mixed solution. The decrease in the liquid film drainage rate correlated with an increase in the PEG content within the mixed solution. This decrease may be attributed to the diminishing hydrophobic attraction between the bubbles. Remarkably, the film drainage rate in the mixed solution was markedly lower than that in the MIBC solution, approaching the film drainage rate observed in the PEG solution. These findings suggested that the incorporation of PEG in small quantities to MIBC can significantly enhance the stability of the liquid film between bubbles. Furthermore, the equilibrium film thickness exhibited a notable increase with a higher PEG component in the mixed solution. As the ratio shifted from 9:1 to 8:2 and 7:3, the equilibrium film thickness increased from 33.10 to 42.17 and 50.02 nm, respectively. The film thickness in the mixed solution was considerably thicker than that in the MIBC solution but thinner than that in the PEG solution. This observation aligns with the results obtained from dynamic foam stability measurements, providing further support for the synergistic effect of the MIBC−PEG combination in froth flotation.

It is widely accepted that pure water is incapable of generating stable bubbles.[38−40] However, the liquid could foam when the liquid is able to form a film around the bubble, which prevents the thinning of liquid film. Conversely, foam cannot form in a pure liquid since there is no mechanism to impede the drainage of the liquid film. Thus, the presence of surface-active molecules, known as surfactant, is necessary for foam formation. These surfactant molecules adsorb at the gas−liquid interface, thereby retarding the drainage of the foam film and creating a mechanically more stable system. The activity of surfactant, is directly related to its ability to reduce surface tension at the gas−liquid interface. This reduction in surface tension occurs as surfactant molecules adsorb at the interface. Moreover, the presence of surfactant molecules enhances the elasticity of the gas−liquid interface, which is attributed to the Marangoni effect. This effect promotes the migration of liquid from regions of low surface tension to those of high surface tension, facilitating the restoration of the thin liquid film to its initial thickness during the drainage process. This phenomenon, known as the self-healing effect of surfactant, effectively prevents bubble coalescence.[41−43]

Under equilibrium conditions and in the absence of external forces, a bubble surface containing a single surfactant (MIBC) tends to exhibit a uniform distribution of surfactant molecules. This arrangement corresponds to a specific surface tension, determined by the concentration of surfactant molecules.

https://doi.org/10.1021/acsomega.3c02863
ACS Omega 2023, 8, 27429−27438

However, any external stimulation to this equilibrium state results in the formation of a surface tension gradient. The introduction of a powerful surfactant molecule (PEG) serves as an external stimulation at the gas−liquid interface, leading to a rearrangement of the surfactant molecules. The powerful surfactant is represented by the open circle with a long chain. This powerful surfactant causes a more significant reduction in local surface tension compared to the weaker surfactant molecules, thereby creating a surface tension gradient. As a result of this surface tension gradient, the weaker surfactant molecules are pushed away from the region occupied by the powerful surfactant molecule. The presence of opposing surface tension gradient forces generates local stresses, as highlighted in studies[26,44] The significant difference in surface tension generates a strong Marangoni flow of surfactant molecules and enhances the self-healing effect at the gas−liquid interface as shown in Figure 11. Consequently, the liquid film drainage rate is reduced, and foam stability is enhanced.

4. CONCLUSIONS

In this study, we focused on the strengthening mechanism of MIBC−PEG mixed surfactant on foam stability. The findings are summarized below:

(1) The surface activity of PEG was found to be higher than that of MIBC, enabling it to reduce tension more effectively than MIBC. Even at low concentrations, the presence of PEG in the mixture resulted in a high surface tension gradient.
(2) Addition of PEG to MIBC enhanced the foaming ability and foam stability of the mixed solution. Moreover, the foaming ability and foam stabilization ability of the mixed solution increased with higher proportions of PEG.
(3) Addition of MIBC and PEG reduced the size of bubbles, primarily by inhibiting bubble coalescence. Notably, PEG exhibited a stronger ability to inhibit bubble coalescence, and its addition to MIBC improved the bubble coalescence inhibition ability of the mixed solution.
(4) Furthermore, the addition of a small amount of PEG to MIBC further slowed down the liquid film drainage rate and enhanced the stability of the liquid film, compare with that in MIBC solution. This can be attributed to the synergistic effect of MIBC and PEG molecules adsorbed at the gas−liquid interface, which effectively delays the liquid film drainage and stabilizes the foam.
(5) The synergistic effect observed between MIBC and PEG is primarily attributed to the significant difference in surface activity between the two molecules, leading to the formation of an additional surface tension gradient. This surface tension gradient, when stimulated externally, intensifies the Marangoni flow of surfactant molecules, thereby enhancing the self-healing effect of the gas−liquid interface and ultimately improving the stability of the liquid film and bubbles.

AUTHOR INFORMATION

Corresponding Author

Yaowen Xing − *Chinese National Engineering Research Center of Coal Preparation and Purification, China University of Mining and Technology, Xuzhou 221116 Jiangsu, China*; Phone: +86-15062114600; Email: cumtxyw@126.com

Authors

Mengdi Xu − *Chinese National Engineering Research Center of Coal Preparation and Purification, China University of Mining and Technology, Xuzhou 221116 Jiangsu, China*

Fangyu Guo − *School of Chemical Engineering and Technology, China University of Mining and Technology, Xuzhou 221116 Jiangsu, China*

Xicheng Bao − *School of Chemical Engineering and Technology, China University of Mining and Technology, Xuzhou 221116 Jiangsu, China*; orcid.org/0000-0001-9421-0946

Xiahui Gui − *Chinese National Engineering Research Center of Coal Preparation and Purification, China University of Mining and Technology, Xuzhou 221116 Jiangsu, China*; orcid.org/0000-0001-9270-7756

Yijun Cao − *Chinese National Engineering Research Center of Coal Preparation and Purification, China University of Mining and Technology, Xuzhou 221116 Jiangsu, China; Henan Province Industrial Technology Research Institute of Resources and Materials, Zhengzhou University, Zhengzhou 450001, China*; orcid.org/0000-0002-4635-0829

Complete contact information is available at: https://pubs.acs.org/10.1021/acsomega.3c02863

Notes

The authors declare no competing financial interest.

ACKNOWLEDGMENTS

This research was funded by the Jiangsu Natural Science Fund-Youth Fund (BK20210500), the National Nature Science Foundation of China (52104277), and the National Nature Science Foundation of China (51920105007).

REFERENCES

(1) Ding, S.; Yin, Q.; Zhang, Y.; He, Q.; Feng, X.; Yang, C.; Cao, Y.; Gui, X.; Xing, Y. Mechanism of the hydrophobic particles with different sizes detaching from the oscillating bubble surface. *Colloids Surf., A* **2022**, *646*, 128986.
(2) Xing, Y.; Xu, M.; Gui, X.; Cao, Y.; Rudolph, M.; Butt, H.; Kappl, M. The role of surface forces in mineral flotation. *Curr. Opin. Colloid Interface Sci.* **2019**, *44*, 143−152.
(3) Li, M.; Xing, Y.; Zhu, C.; Liu, Q.; Yang, Z.; Zhang, R.; Zhang, Y.; Xia, Y.; Gui, X. Effect of roughness on wettability and floatability: Based on wetting film drainage between bubbles and solid surfaces. *Int. J. Min. Sci. Technol.* **2022**, *32*, 1389−1396.
(4) Xing, Y.; Gui, X.; Pan, L.; Pinchasik, B.; Cao, Y.; Liu, J.; Kappl, M.; Butt, H. Recent experimental advances for understanding bubble-particle attachment in flotation. *Adv. Colloid Interface Sci.* **2017**, *246*, 105−132.
(5) Xing, Y.; Gui, X.; Cao, Y.; Wang, D.; Zhang, H. Clean low-rank-coal purification technique combining cyclonic-static microbubble flotation column with collector emulsification. *J. Cleaner Prod.* **2017**, *153*, 657−672.
(6) Zhang, R.; Xing, Y.; Xia, Y.; Guo, F.; Ding, S.; Tan, J.; Che, T.; Meng, F.; Gui, X. Synergistic adsorption mechanism of anionic and cationic surfactant mixtures on low-rank coal flotation. *ACS Omega* **2020**, *5*, 20630−20637.
(7) Ata, S. Phenomena in the froth phase of flotation—A review. *Int. J. Miner. Process.* **2012**, *102−103*, 1−12.
(8) Schwarz, S.; Grano, S. Effect of particle hydrophobicity on particle and water transport across a flotation froth. *Colloids Surf., A* **2005**, *256*, 157−164.
(9) Bera, A.; Ojha, K.; Mandal, A. Synergistic effect of mixed surfactant systems on foam behavior and surface tension. *J. Surfactants Deterg.* **2013**, *16*, 621−630.

(10) Farrokhpay, S. The significance of froth stability in mineral flotation-A review. *Adv. Colloid Interface Sci.* **2011**, *166*, 1−7.
(11) Kang, H.; Zhang, H. Enhanced flotation separation of low-rank coal with a mixed collector: experimental and molecular dynamics simulation study. *ACS Omega* **2022**, *7*, 34239−34248.
(12) McFadzean, B.; Marozva, T.; Wiese, J. Flotation frother mixtures: Decoupling the sub-processes of froth stability, froth recovery and entrainment. *Miner. Eng.* **2016**, *85*, 72−79.
(13) Cheng, Y.; Min, F.; Li, H.; Chen, J.; Fu, X. Effect of reagent interaction on froth stability of coal flotation. *Fuel* **2022**, *318*, 123417.
(14) He, J.; Liu, G.; Sang, G.; He, J.; Wu, Y. Investigation on foam stability of multi-component composite foaming agent. *Constr. Build. Mater.* **2023**, *391*, 131799.
(15) Saavedra Moreno, Y.; Bournival, G.; Ata, S. Foam stability of flotation frothers under dynamic and static conditions. *Sep. Purif. Technol.* **2021**, *274*, 117822.
(16) Alexander, S.; Barron, A.; Denkov, N.; Grassia, P.; Kiani, S.; Sagisaka, M.; Shojaei, M.; Shokri, N. Foam generation and stability: role of the surfactant structure and asphaltene aggregates. *Ind. Eng. Chem. Res.* **2022**, *61*, 372−381.
(17) Li, C.; Cao, Y.; Peng, W.; Shi, F. On the correlation between froth stability and viscosity in flotation. *Miner. Eng.* **2020**, *149*, 106269.
(18) Kawale, D.; van Nimwegen, A.; Portela, L.; van Dijk, M.; Henkes, R. The relation between the dynamic surface tension and the foaming behaviour in a sparger setup. *Colloids Surf., A* **2015**, *481*, 328−336.
(19) Langevin, D.; Monroy, F. Marangoni stresses and surface compression rheology of surfactant solutions. Achievements and problems. *Adv. Colloid Interface Sci.* **2014**, *206*, 141−149.
(20) Novev, J.; Panchev, N.; Slavchov, R. Evaporating foam films of pure liquid stabilized via the thermal Marangoni effect. *Chem. Eng. Sci.* **2017**, *171*, 520−533.
(21) Cho, Y.; Laskowski, J. Effect of flotation frothers on bubble size and foam stability. *Int. J. Miner. Process.* **2002**, *64*, 69−80.
(22) Grau, R.; Laskowski, J.; Heiskanen, K. Effect of frothers on bubble size. *Int. J. Miner. Process.* **2005**, *76*, 225−233.
(23) Laskowski, J.; Tlhone, T.; Williams, P.; Ding, K. Fundamental properties of the polyoxypropylene alkyl ether flotation frothers. *Int. J. Miner. Process.* **2003**, *72*, 289−299.
(24) Gupta, A.; Banerjee, P.; Mishra, A. Influence of chemical parameters on selectivity and recovery of fine coal through flotation. *Int. J. Miner. Process.* **2009**, *92*, 1−6.
(25) Tan, S. N.; Pugh, R.; Fornasiero, D.; Sedev, R.; Ralston, J. Foaming of polypropylene glycols and glycol/MIBC mixtures. *Miner. Eng.* **2005**, *18*, 179−188.
(26) Dey, S.; Pani, S.; Singh, R. Study of interactions of frother blends and its effect on coal flotation. *Powder Technol.* **2014**, *260*, 78−83.
(27) Xu, M.; Xing, Y.; Jin, W.; Li, M.; Cao, Y.; Gui, X. Effect of diesel on the froth stability and its antifoam mechanism in fine coal flotation used MIBC as the frother. *Powder Technol.* **2020**, *364*, 183−188.
(28) Xing, Y.; Gui, X.; Cao, Y.; Wang, Y.; Xu, M.; Wang, D.; Li, C. Effect of compound collector and blending frother on froth stability and flotation performance of oxidized coal. *Powder Technol.* **2017**, *305*, 166−173.
(29) Zanin, M.; Wightman, E.; Grano, S.; Franzidis, J. Quantifying contributions to froth stability in porphyry copper plants. *Int. J. Miner. Process.* **2009**, *91*, 19−27.
(30) Barbian, N.; Hadler, K.; Cilliers, J. The froth stability column: Measuring froth stability at an industrial scale. *Miner. Eng.* **2006**, *19*, 713−718.
(31) Bikerman, J. *Foams*; Springer-Verlag: Berlin, 1973.
(32) Barigou, M.; Deshpande, N.; Wiggers, F. An enhanced electrical resistance technique for foam drainage measurement. *Colloids Surf., A* **2001**, *189*, 237−246.
(33) Cheng, Y.; Min, F.; Li, H.; Chen, J.; Fu, X. Effect of reagent interaction on froth stability of coal flotation. *Fuel* **2022**, *318*, 123417.
(34) Tse, K.; Martin, T.; Mcfarlane, C.; Nienow, A. Small bubble formation via a coalescence dependent break-up mechanism. *Chem. Eng. Sci.* **2003**, *58*, 275−286.
(35) Israelachvili, J.; Mcguiggan, P.; Homola, A. Dynamic properties of molecularly thin liquid films. *Science* **1988**, *240*, 189−191.
(36) Yoon, R.; Aksoy, B. Hydrophobic forces in thin water films stabilized by dodecylammonium chloride. *J. Colloid Interface Sci.* **1999**, *211*, 1−10.
(37) Angarska, J.; Dimitrova, B.; Danov, K.; Kralchevsky, P.; Ananthapadmanabhan, K.; Lips, A. Detection of the hydrophobic surface force in foam films by measurements of the critical thickness of the film rupture. *Langmuir* **2004**, *20*, 1799−1806.
(38) Lessard, R.; Zieminski, S. Bubble coalescence and gas transfer in aqueous electrolyte solutions. *Ind. Eng. Chem. Fundam.* **1971**, *10*, 260−269.
(39) Christenson, H.; Bowen, R.; Carlton, J.; Denne, J.; Lu, Y. Electrolytes that show a transition to bubble coalescence inhibition at high concentrations. *J. Phys. Chem. C* **2008**, *112*, 794−796.
(40) Karakashev, S.; Firouzi, M.; Wang, J.; Alexandrova, L.; Nguyen, A. On the stability of thin films of pure water. *Adv. Colloid Interface Sci.* **2019**, *268*, 82−90.
(41) Tan, S.; Fornasiero, D.; Sedev, R.; Ralston, J. Marangoni effects in aqueous polypropylene glycol foams. *J. Colloid Interface Sci.* **2005**, *286*, 719−729.
(42) Gordeeva, V.; Lyushnin, A. Dynamics of an evaporating thin film of polar liquid with solutocapillary Marangoni effect and capillary osmosis. *Surf. Coat. Technol.* **2017**, *320*, 531−535.
(43) Dunér, G.; Kim, M.; Tilton, R.; Garoff, S.; Przybycien, T. Effect of polyelectrolyte−surfactant complexation on Marangoni transport at a liquid−liquid interface. *J. Colloid Interface Sci.* **2016**, *467*, 105−114.
(44) Wang, L.; Yoon, R. Effects of surface forces and film elasticity on foam stability. *Int. J. Miner. Process.* **2008**, *85*, 101−110.

https://doi.org/10.1021/acsomega.3c02863
ACS Omega 2023, 8, 27429−27438